JOURNAL OF GUIDANCE, CONTROL, AND DYNAMICS
Vol. 19, No. 4, July–August 1996

Multivariable Control of the J-85 Turbojet Engine for Full Flight Envelope Operation

Shih-Tin Lin and Chun-Mo Lee
National Chung-Hsing University, Taichung 40227, Taiwan, Republic of China

The design of a J-85 turbojet engine controller using Edmunds' method and gain scheduling techniques is presented. A nonlinear engine model was first linearized at 50 selected operating points throughout the flight power envelope of the J-85 engine. The operating points were selected based on the engine's altitude, Mach number, and compressor rotor speed. Edmunds' method was then used to design a linear controller for each operating point. The objective of this method is to design a simple controller, which achieves a desired performance criteria. Finally, for full flight envelope operation, two gain scheduling approaches were evaluated: 1) extended Kalman filter and 2) neural networks. The objectives of this research are to evaluate Edmunds' method for the design of a J-85 engine controller, as well as gain scheduling approaches for the full flight power envelope operation. After completing the controller design for 50 operation points, we found that Edmunds' method is very effective for this application. For the gain scheduling approaches, simulation results show that the controller using neural networks has better performance.

Introduction

FROM a control viewpoint, a modern engine can be considered as a nonlinear multiple input multiple output (MIMO) system. If a traditional single input single output (SISO) method is used to design the controller, control function for each input is designed independently. When these independently designed control functions are combined into a complete engine controller, input/output interaction may degrade the engine performance. Because of this characteristic, it is difficult for a traditional SISO control method to meet the desired performance criteria. Modern MIMO control methods are considered a better approach.

Several multivariable feedback control design techniques have been used to design control systems for jet engines. Dehoff et al.[1] applied the linear quadratic regulator method to F-100 engine control design. Pfeil et al.[2] used the linear quadratic Gaussian/loop transfer recovery (LQG/LTR) method for a General Electric (GE) T700 engine control design. Athans et al.[3] used the same method in the F-100 engine. Polley et al.[4] used Edmunds' technique[5] in GE16/J11A6 engine control design. Moellenhoff et al.[6] combined the LQG/LTR and parameter robust linear quadratic Gaussian methods to design a robust engine controller. This research studied the design of a multivariable compensator for a single operating point. Kapasouris[7] used a gain scheduling technique in a GE-21 engine control design. However, the only scheduled variable considered in this paper is the low-pressure rotor speed. Polley et al.[8] extended his previous work by using Edmunds' technique[5] with gain scheduling to design a nonlinear multivariable controller that operates over the entire flight envelope of the GE 16/J11A6 engine.

Edmunds' method[5] and gain scheduling techniques are used in this paper to design a controller for a J-85 turbojet engine for full flight envelope operation. Edmunds' method is a linear multivariable design method, which uses closed-loop Nyquist and Bode arrays. The parameters of the controller are adjusted so that the closed-loop frequency response is as close as possible, in a least square sense, to a desired response. Advantages of Edmunds' method are that it is conceptually simple, easy to use, and allows the user to develop controllers that are easy to implement. This paper emphasizes the

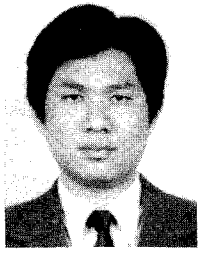

Shih-Tin Lin received his B.S. degree in Mechanical Engineering from Tatung Institute of Technology, Taiwan, in 1984 and his M.S. and Ph.D. in Mechanical Engineering from the University of Iowa in 1988 and 1992, respectively. He is currently Associate Professor in the Department of Mechanical Engineering at the National Chung-Hsing University, Taichung, Taiwan. Research interests include robotics, linear and nonlinear control, intelligent control, and simulation of multibody dynamics and kinematics.

Chun-Mo Lee received his B.S. degree from the Institute of Aeronautics and Astronautics of the National Cheng Kung University, Taiwan, in 1993 and his M.S. in the Department of Mechanical Engineering from the National Chung-Hsing University, Taiwan, in 1995. He is currently an engineer at the China Motor Corporation, Taiwan. His research interests are linear and nonlinear control, and intelligent control.

Received Aug. 25, 1995; revision received Jan. 7, 1996; accepted for publication Jan. 13, 1996.

choice of the desired response, which greatly affects the success of Edmunds' method.

To design a controller for full flight envelope operation, Edmunds' method was first applied to design a linear controller at 50 selected design operating points. Two approaches were used to schedule controller's gains for full flight envelope operation, the extended Kalman filter (EKF) and neural networks. In the EKF approach, the controller's gains were assumed to be power functions of the engine's altitude, Mach number, and compressor rotor speed with unknown power parameters estimated by the EKF. In this method, a nonlinear system is first linearized around the current estimates of the unknown parameters and the Kalman filter is then applied to the resulting linear system. The disadvantage of this method is that the relationship between the controller's gains and the scheduling variables is not necessarily a power function. If this is the case, adding more design operating points or using different identification methods will not improve the performance of the gain scheduling.

In this paper, artificial neural networks are used to avoid this problem. Although applications of neural networks for aircraft have been studied in recent years, most have focused primarily on flight control.[9–11] In this paper, neural networks are used to schedule the controller's gains of a J-85 turbojet engine for full flight envelope operation. Neural networks have been shown to be a powerful tool for identification of systems with unknown nonlinearities.[12] The mapping between inputs and outputs of a system is learned by adjusting weights between connecting neurons. Therefore, we do not need to search for suitable nonlinear function to approximate the mapping of engine's altitude, Mach number, and compressor rotor speed into the controller's gains.

Edmunds' Method

The objective of Edmunds' method is to design a simple-structure controller so that the closed-loop frequency response is as close as possible to a desired response over a specified frequency range. The controller's optimal parameters can be obtained by minimizing a quadratic error function pointwise over the specified frequency range. The problem can be posed as a linear least square problem to which a standard solution is known. Details of this method can be found in Maciejowski.[13] The rest of this section summarizes important design steps of Edmunds' method.

Choice of the Desired Closed-Loop Transfer Function

A key issue with Edmunds' method concerns proper selection of the desired closed-loop transfer function matrix T_t. It is possible to cause a large error between T, the actual closed-loop transfer function, and T_t or to cause the closed-loop system to be unstable, if an improper T_t is chosen. Choice of T_t consists of the following steps:

1)T_t is usually a diagonal matrix, which means that the desired closed-loop response is decoupled,

$$T_t(s) = \begin{bmatrix} t_{11} & \cdots & 0 \\ \vdots & \ddots & \vdots \\ 0 & \cdots & t_{hh} \end{bmatrix} \tag{1}$$

2) The order difference of diagonal elements of T_t must be determined by the number of infinite zeros of the plant G and the compensator K. This can be shown as follows.

Suppose the transfer functions of the plant G and compensator K are

$$G(s) = \begin{bmatrix} g_{11} & \cdots & g_{1m} \\ \vdots & & \vdots \\ g_{h1} & \cdots & g_{hm} \end{bmatrix} = \begin{bmatrix} g_1 \\ \vdots \\ g_h \end{bmatrix} \tag{2}$$

$$K(s) = \begin{bmatrix} k_{11} & \cdots & k_{1h} \\ \vdots & & \vdots \\ k_{m1} & \cdots & k_{mh} \end{bmatrix} = [k_1 \quad \cdots \quad k_h] \tag{3}$$

where $g_i = [g_{i1} \ \cdots \ g_{im}]$ and $k_i = [k_{1i} \ \cdots \ k_{mi}]^T$. From Eqs. (2) and (3), we know

$$G(s)K(s) = \begin{bmatrix} g_1k_1 & \cdots & g_1k_h \\ \vdots & \ddots & \vdots \\ g_hk_1 & \cdots & g_hk_h \end{bmatrix} \tag{4}$$

Suppose the actual closed-loop transfer function T is

$$T(s) = \begin{bmatrix} \hat{t}_{11} & \cdots & 0 \\ \vdots & \ddots & \vdots \\ 0 & \cdots & \hat{t}_{hh} \end{bmatrix} \tag{5}$$

then

$$GK = T(s)[I - T(s)]^{-1} = \begin{bmatrix} \dfrac{\hat{t}_{11}}{1-\hat{t}_{11}} & \cdots & 0 \\ \vdots & \ddots & \vdots \\ 0 & \vdots & \dfrac{\hat{t}_{hh}}{1-\hat{t}_{hh}} \end{bmatrix} \tag{6}$$

From Eqs. (4) and (6), we obtain

$$\begin{bmatrix} \hat{t}_{11} = \dfrac{g_1k_1}{1+g_1k_1} \\ \vdots \\ \hat{t}_{hh} = \dfrac{g_hk_h}{1+g_hk_h} \end{bmatrix} \tag{7}$$

In Edmunds' method, the error function $E = T_t - T$ is minimized in the frequency domain. To have a good match between T_t and T, one should ensure that the rolloff rate of T_t at high frequencies is compatible with that of T. Elements of K are usually chosen to have the same number of infinite zeros for simplicity. If the number of infinite zeros of each of the elements of K is n, from Eq. (7) we observe that the number of infinite zeros of $\hat{t}_{ii}$ will be equal to that of g_i plus n. Here the number of infinite zeros of g_i is defined as the minimum value of the set $g_i = [g_{i1} \ \cdots \ g_{im}]$. Because the rolloff rate of T_t at high frequencies should be the same as that of T, the number of infinite zeros of t_{ii} should be the same as that of $\hat{t}_{ii}$.

3) The pole position of T_t depends on the desired response speed. The desired speed cannot be too fast to avoid actuator saturation and other physical limits.

4) If G has any right half-plane zeros, T_t must preserve these right half-plane zeros.[13] In SISO systems, unless there is pole-zero cancellation, the closed-loop systems will preserve zeros of the plant. If G has a right half-plane zero and T_t does not, then GK_t has an unstable pole-zero cancellation. K_t is a target controller such that

$$GK_t = T_t(I - T_t)^{-1} \tag{8}$$

In this case, although the Nyquist plot of GK_t shows the closed-loop stability of the system, the system will have unstable internal dynamics. In Edmunds' method, the actual GK is only approximate to the desired GK_t, and so the unstable pole-zero cancellation will not really happen. Therefore, the designed controller usually gives an unstable closed-loop system.

Nett[13] extended this idea to MIMO systems. In MIMO systems, the role of zeros is replaced by transmission zeros and the Nyquist plot is replaced by the characteristics loci plot.

Choice of the Controller's Structure

The lower the order of the denominator of K, the easier it is for the controller K to be implemented. In contrast, the higher the order of the numerator, the easier it is for Edmunds' method to obtain a good match between T and T_t. Since the order of the numerator can not be greater than that of denominator, designers must consider these two counter effects simultaneously. If high precision between T and T_t is desired, then a high-order numerator and denominator

are needed. In contrast, if a simple-structure controller is desired, then a low-order denominator and numerator are needed.

The rolloff rates of the gain-frequency for elements of K_t are used to choose the pole positions of K. For instance, if the rolloff rates of K_t are -20 dB/decade at low frequency, then K preserves the pole ($s = 0$), and if the rolloff rates of K_t are added -20 dB/decade at $s = -\omega$, then K preserves the pole ($s = -\omega$).

Choice of the Scaling Matrix

Since the system output responses are usually of different magnitude, a scaling matrix S must be used so that the steady-state gains have similar magnitudes for all of the outputs. A suitable scaling matrix can be obtained by referring to the step responses of the plant.

Choice of the Weighting Matrix

A weighting matrix W can be attached to the error function to emphasize the attainment of certain elements of T_t, at the expense of others. For example, if the decoupled effect is emphasized, then the off-diagonal elements of W should be larger than the diagonal elements of W. In addition, one can apply different weights at different frequencies.

Performance Requirements

The performance requirements considered in this engine controller design are as follows: settling time is close to the desired value and minimizing the overshoot, minimizing the coupling effect, low-frequency command following, low-frequency disturbance rejection, and insensitivity to high-frequency sensor noise. The last three requirements can be achieved by making $\sigma_{\min}(GK)$ large at low frequency and $\sigma_{\max}(GK)$ small at high frequency.[14]

Controller Design for an Operating Point of the J-85 Engine by Edmunds' Method

For the design points for full flight envelope operation 50 engine operating points were selected. An operating point at altitude = 0, Mach = 0, and N = 13,200 rpm is chosen here to demonstrate the design procedure of Edmunds' method. The nonlinear engine model[15] was first linearized at this operating point. The resulting linear model has eight states, three inputs, and three outputs. The inputs are main fuel flow rate ($\Delta \dot{W}f$), bleed flow rate (ΔBLD), and nozzle jet area ($\Delta A8$). The outputs are compressor discharge pressure ($\Delta P3$), turbine inlet temperature ($\Delta T4$), and compressor speed (ΔN). The overall system block diagram is shown in Fig. 1. The objective of the controller is to indirectly control thrust while maintaining adequate fan and compressor stall margins and also to maintain engine temperature within the acceptable limits.

The following design steps were all done using MATLAB. From the A, B, C, and D matrices of the linearized model, a 3 × 3 transfer function G can be obtained.

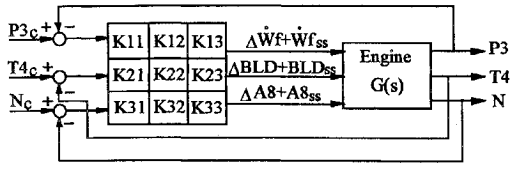

Fig. 1 Block diagram of the closed-loop system.

Choice of Closed-Loop Transfer Function

Choice of the desired closed-loop transfer function T_t consists of the following steps:

1) The minimum order difference for each row of G is $g_1 = 2$, $g_2 = 1$, $g_3 = 2$. For simplicity, we choose the order difference for $t_{11} = t_{22} = t_{33} = 2$. 2) Suppose the desired settling time is 1 s and choose two dominant poles; $s = -10, -10$ accordingly. 3) Suppose that the off-diagonal elements of $T_t(s)$ are zero, so as to make the closed-loop system decoupled.

From these three steps, we can choose

$$T_d(s) = [10/(s+10)]^2 I \tag{9}$$

where I is a 3 × 3 identity matrix.

Choice of Controller's Structure

Since the controller was designed for full flight operation, we must use a common denominator of the compensator K for different operating points. After several trials, a third-order controller with poles at 0, -4, and -16 was used:

$$K(s) = \begin{bmatrix} \dfrac{v_{113}s^3 + v_{112}s^2 + v_{111}s + v_{110}}{s(s+4)(s+16)} & \cdots & \dfrac{v_{133}s^3 + v_{132}s^2 + v_{131}s + v_{130}}{s(s+4)(s+16)} \\ \vdots & \ddots & \vdots \\ \dfrac{v_{313}s^3 + v_{312}s^2 + v_{311}s + v_{310}}{s(s+4)(s+16)} & \cdots & \dfrac{v_{333}s^3 + v_{332}s^2 + v_{331}s + v_{330}}{s(s+4)(s+16)} \end{bmatrix} \tag{10}$$

Choice of the Scaling Matrix

From step responses of the uncontrolled engine, we can choose the scaling matrix as

$$S = \text{diag}\left[\frac{1}{0.7}, \frac{1}{2.7}, \frac{1}{7.8}\right] \tag{11}$$

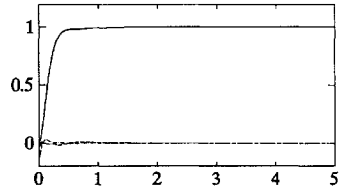

Unit step response of $p3$

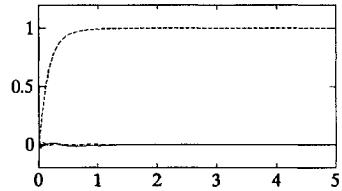

Unit step response of $t4$

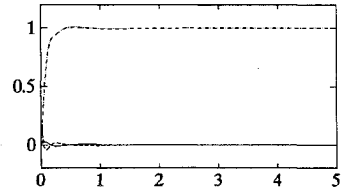

Unit step response of N

Fig. 2 Closed-loop unit step responses of the scaled outputs: ——, $p3$ (psi); – –, $t4$(°R); and –·–, N (rpm).

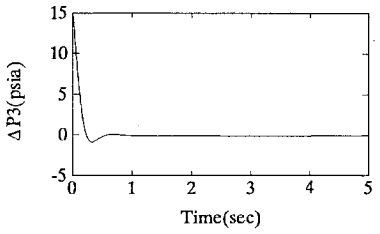

Pressure of compressor

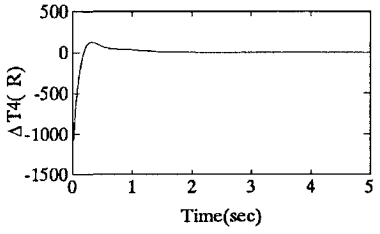

Fan tribune inlet temperature

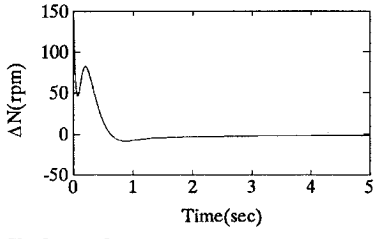

Shaft speed

Fig. 3 Closed-loop response of the outputs for sea level static $N = 13{,}200$ rpm.

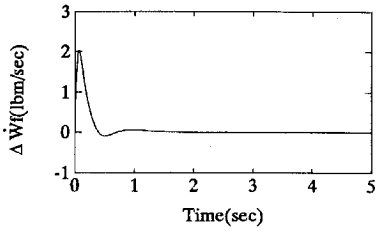

Main fuel flow

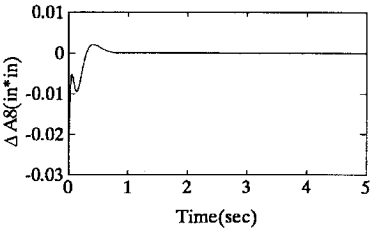

Nozzle jet area

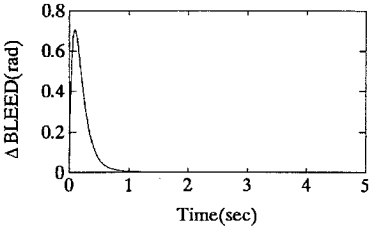

Fan guide vane

Fig. 4 Controller outputs for altitude = 0, Mach = 0, and $N = 13{,}200$ rpm.

Choice of the Weighting Matrix

Choosing

$$W = \frac{1}{s+1}\begin{bmatrix} 1 & 1000 & 1000 \\ 1000 & 1 & 1000 \\ 1000 & 1000 & 1 \end{bmatrix} \tag{12}$$

The off-diagonal entries were set to be 1000 to emphasize the decoupling effect. The low-pass filter increases weights at low frequency.

Analysis of the Closed-Loop System

After the design steps were complete, the numerator coefficients of the tuned controller can be calculated using Edmunds' technique. We can analyze the results as follows.

The closed-loop unit step responses of the scaled outputs are shown in Fig. 2, which shows that the settling times are about 1 s with almost no coupling effect observed; only a little overshoot is observed in the response of $\Delta P3$.

The singular value plots of GK show that low frequency: $\sigma_{\min}[GK] \gg 1$ and high frequency: $\sigma_{\max}[GK] \ll 1$.

For the steady-state control mode if the engine's outputs are perturbed from their steady-state values, Fig. 3 shows that the controller can drive the engine's outputs back to the steady-state values in about 1 s. Figure 4 shows the controller outputs.

Full Flight Envelope Design

The J-85 engine's operating points are represented by its altitude, Mach number, and compressor speed. To cover the flight envelope, 50 operating points were chosen. These operating points were separated into five power levels (80, 85, 90, 95, and 100% of the maximum compressor speed); each power level has 10 operating points. Details of the operating points and corresponding steady-state values are listed in Table 1: Alt is altitude, $T0$ and $P0$ are ambient temperature and pressure, respectively, and Mach is, of course, Mach number. Note that there are many possible combinations of control inputs to reach a desired operating point. In this research, we fixed the values of bleed flow rate to 0 and nozzle jet area to 162 to find a unique solution of main fuel flow rate at each operating point.

Edmunds' method was used to design a linear controller for each operating point. The compensator K for each operating point has the same denominator but different numerator coefficients. Two different approaches, an EKF and a neural network, were used to determine the numerator coefficients of the compensator K for every operating point in the flight envelope. In the EKF, the unknown coefficients are assumed to be power functions of the scheduled variables, that is,

$$V_{ijk} = K_{ijk}[M]^{a_{ijk}}[H]^{b_{ijk}}[N]^{c_{ijk}} = f(M, H, N, \theta) \tag{13}$$

where V_{ijk} are the numerator coefficients; M, H, and N are Mach number, altitude, and compressor speed, respectively; $K_{ijk}, a_{ijk}, b_{ijk}$, and c_{ijk} are the unknown parameters; and $\theta = (K_{ijk}, a_{ijk}, b_{ijk}, c_{ijk})^T$.

Since power functions are nonlinear, the EKF is used to identify the unknown parameters K_{ijk}, a_{ijk}, b_{ijk}, and c_{ijk}. In this method, the nonlinear system [Eq. (13)] is first linearized around the current estimate and the Kalman filter is then applied to the resulting linear system. Suppose the current estimate is $\hat{\theta}(n)$; then the formulation of the EKF is

$$\begin{aligned} \hat{\theta}(n+1) &= \hat{\theta}(n) + P(n)\{V_{ijk}(n) - f[M(n), N(n), H(n), \hat{\theta}(n)]\} \\ P(n) &= E(n)\phi^T(n)[R + \phi(n)E(n)\phi^T(n)]^{-1} \\ E(n+1) &= E(n) - P(n)\phi(n)E(n) \end{aligned} \tag{14}$$

where

$$\phi^T(n) = \left.\frac{\partial f}{\partial \theta}\right|_{\theta=\hat{\theta}(n)} = [d_1 \quad d_2 \quad d_3 \quad d_4]^T$$

$$\begin{aligned} d_1 &= [M(n)]^{\hat{a}_{ijk}(n)}[H(n)]^{\hat{b}_{ijk}(n)}[N(n)]^{\hat{c}_{ijk}(n)} \\ d_2 &= \hat{K}_{ijk}(n)[M(n)]^{\hat{a}_{ijk}(n)}[H(n)]^{\hat{b}_{ijk}(n)}[N(n)]^{\hat{c}_{ijk}(n)}\ell_n[M(n)] \\ d_3 &= \hat{K}_{ijk}(n)[M(n)]^{\hat{a}_{ijk}(n)}[H(n)]^{\hat{b}_{ijk}(n)}[N(n)]^{\hat{c}_{ijk}(n)}\ell_n[H(n)] \\ d_4 &= \hat{K}_{ijk}(n)[M(n)]^{\hat{a}_{ijk}(n)}[H(n)]^{\hat{b}_{ijk}(n)}[N(n)]^{\hat{c}_{ijk}(n)}\ell_n[N(n)] \end{aligned} \tag{15}$$

Table 1 Operating points

Point	Alt ($\times 10^3$ft)	$\dot{W}_f$, lbm/s	$P3$, psi	$T4$, °R	$T0$, °R	$P0$, psi	Mach
		Speed N = 13,200 rpm (80% of max. spool speed)					
1	0	996	46.70	1688.90	518.7	14.69	0.00
2	0	4035	157.46	2306.30	518.7	14.69	1.48
3	10	667	32.74	1553.80	483.0	10.11	0.20
4	10	4029	150.09	2398.47	483.0	10.11	1.71
5	20	450	24.60	1413.92	447.4	6.76	0.50
6	20	3922	140.29	2485.47	447.4	6.76	1.94
7	30	322	19.81	1297.35	411.8	4.37	0.80
8	30	3938	133.10	2610.90	411.8	4.37	2.20
9	40	304	19.23	1353.70	390.0	2.73	1.20
10	40	3215	105.08	2684.48	390.0	2.73	2.36
		Speed N = 14,025 rpm (85% of max. spool speed)					
1	0	1310	62.14	1753.69	518.7	14.69	0.00
2	0	4028	149.09	2310.26	518.7	14.69	1.19
3	10	860	43.68	1619.07	483.0	10.11	0.20
4	10	3941	140.66	2386.42	483.0	10.11	1.43
5	20	609	33.22	1509.03	447.4	6.76	0.50
6	20	3912	133.63	2484.54	447.4	6.76	1.68
7	30	482	27.30	1452.15	411.8	4.37	0.80
8	30	3547	118.60	2533.33	411.8	4.37	1.90
9	40	475	25.37	1554.60	390.0	2.73	1.15
10	40	3236	101.25	2687.53	390.0	2.73	2.11
		Speed N = 14,850 rpm (90% of max. spool speed)					
1	0	1676	77.70	1825.50	518.7	14.69	0.00
2	0	3913	146.14	2264.07	518.7	14.69	0.98
3	10	1112	55.09	1697.57	483.0	10.11	0.22
4	10	3819	138.02	2333.07	483.0	10.11	1.24
5	20	826	42.60	1621.15	447.4	6.76	0.52
6	20	3765	130.76	2421.93	447.4	6.76	1.50
7	30	674	34.89	1593.03	411.8	4.37	0.80
8	30	3855	126.03	2556.03	411.8	4.37	1.78
9	40	717	34.51	1741.66	390.0	2.73	1.20
10	40	3415	105.74	2686.50	390.0	2.73	1.98
		Speed N = 15,675 rpm (95% of max. spool speed)					
1	0	2340	91.92	2077.94	518.7	14.69	0.00
2	0	5546	172.16	2609.10	518.7	14.69	0.97
3	10	1542	64.77	1934.64	483.0	10.11	0.20
4	10	5289	160.29	2670.66	483.0	10.11	1.22
5	20	1259	53.69	1902.12	447.4	6.76	0.60
6	20	4599	139.06	2676.86	447.4	6.76	1.42
7	30	944	41.40	1834.05	411.8	4.37	0.80
8	30	3912	118.26	2677.55	411.8	4.37	1.62
9	40	1007	40.96	2003.84	390.0	2.73	1.20
10	40	2877	87.45	2667.05	390.0	2.73	1.74
		Speed N = 16,500 rpm (100% of max. spool speed)					
1	0	3207	106.89	2378.16	518.7	14.69	0.00
2	0	3912	123.50	2507.57	518.7	14.69	0.45
3	10	2108	75.25	2210.78	483.0	10.11	0.20
4	10	3889	119.07	2587.58	483.0	10.11	0.85
5	20	1560	57.93	2123.18	447.4	6.76	0.50
6	20	3855	114.06	2679.55	447.4	6.76	1.16
7	30	1279	48.10	2096.20	411.8	4.37	0.80
8	30	3308	97.71	2685.33	411.8	4.37	1.38
9	40	1368	47.61	2290.45	390.0	2.73	1.20
10	40	2503	73.77	2696.15	390.0	2.73	1.52

Filter tuning is necessary for satisfactory convergence of unknown parameters. In this case, filter tuning consists of the selection of $\hat{\theta}(0)$, $P(0)$, and R. Here, $\hat{\theta}(0)$ are the initial estimates of the unknown parameters. Since no prior knowledge about the unknown parameters are available, estimates of the unknown parameters start at zero. The magnitude of $P(0)$ affects the transient of the estimates. A large $P(0)$ produces large initial transient and fast convergence, whereas a small $P(0)$ has the opposite effect. The magnitude of R has the same effect as $P(0)$. The sizes of $P(0)$ and R are adjusted by trial and error until satisfactory behavior is achieved.

In the neural network approach, nine feedforward error-back propagation neural networks were used to learn the nonlinear mapping between the compensator numerator coefficients and the scheduled variables. The structure of the neural network is shown in Fig. 5. Figure 5 shows that the neural network consists of four layers, including input/output layers and two hidden layers. The input to a hidden layer or output layer node is a weighted sum of the previous layer. This sum is passed through a nonlinear activation function $f(x)$. The input–output relationship of neuron unit are as follows:

$$\text{net}_i = \sum_{j=1}^{n} w_{ij} o_j \tag{16}$$

$$o_i = f(\text{net}_i) \tag{17}$$

where net_i is the state of unit i, w_{ij} is the interconnection weight

Table 2 Test points

Test point	Alt	$\dot{W}f$	A8	*BLD*	*N*	*P*3	*T*4	*T*0	Mach
1	0	801	162	0	13,200	48.04	1596	6.76	1.2
2	0	1020	162	0	14,025	52.84	1713	6.76	1

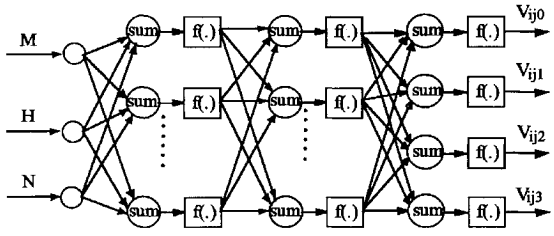

Fig. 5 Structure of the neural network.

between units j and i, and o_i in the output of unit i. In this paper, a typical continuous activation function

$$f(x) = \frac{1 - \exp(-x)}{1 + \exp(-x)} \tag{18}$$

is used. The input layer has three nodes and the output layer has four nodes. Input data consists of Mach number, altitude, and compressor speed. Output data consist of the coefficients of the numerator for each entry of the compensator K.

The neural networks were trained using the generalized δ rule (Ref. 16) and the parameters from the linear controllers designed for the 50 operating points using Edmunds' method. The weight between the ith and jth unit is changed by the following equation:

$$w_{ij}(k) = w_{ij}(k-1) + \eta \cdot \delta_i \cdot o_j \tag{19}$$

where η is the learning rate and δ_i is given by the following equation for output units:

$$\delta_i = (d_i - o_i) f'(\text{net}_i) \tag{20}$$

and for other units:

$$\delta_i = f'(\text{net}_i) \sum_k w_{ki} \delta_k \tag{21}$$

where d_i is the desired output of the unit, $f'(\cdot)$ is the derivative of the function $f(\cdot)$ with respect to net, and k denotes the number of units in the succeeding layer. Weights of each neural network start at a random number between 1 and -1.

In this paper, a neural network is used for each entry of K. As a result, nine neural networks are required to identify all of the coefficients of the numerators of the compensator K. If only one neural network is used to identify all of the coefficients, the output layer of the neural network will have 36 nodes. Training of such neural networks will be computationally slow because of the complexity of the structure of the neural network. Another disadvantage of using only one neural network is that the convergent solution of the neural network is hard to find.

Two test points, which were not included in the 50 design points, were used to test the performance of the proposed controller. The corresponding scheduled variables and the steady-state values of these two test points are listed in Table 2. Simulation results for steady-state control using the EKF and neural networks are shown in Figs. 6–8 and 9–11, respectively, for perturbation of the outputs from the steady-state values. Figures 6 and 9 show that the controller using either scheduling method can drive the engine back to its steady-state values within 1–2 s when the engine is operating around test point 1. However, Figs. 7 and 10 show that the responses of the system using the EKF scheduling method have longer settling times than those using the neural networks, especially in the response of ΔN when the engine is operating around test point 2. Figures 8 and 11 show the controller outputs of the system using the EKF and the neural network technique, respectively, when the engine is operating around test point 1. Simulation results for several other

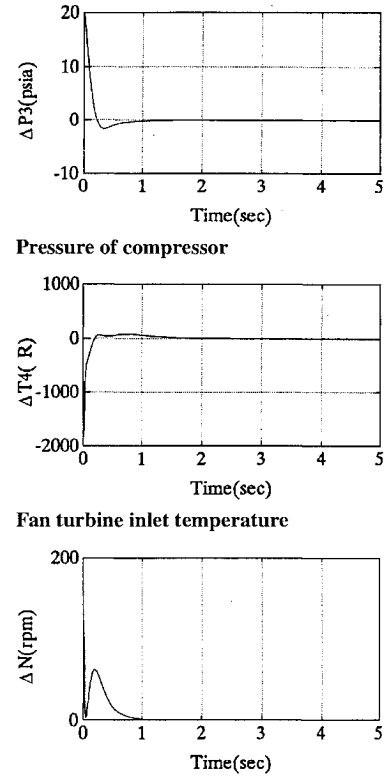

Fig. 6 Closed-loop response of the outputs for test point 1 using EKF.

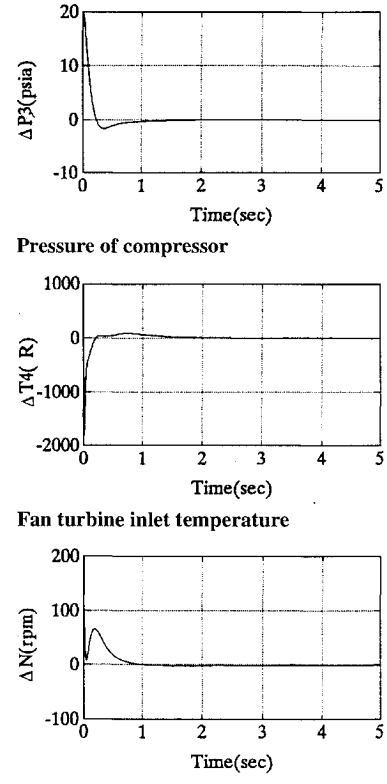

Fig. 7 Closed-loop response of the outputs for test point 2 using EKF.

testing points all indicate that the performance of the system using the neural networks is equal or better than the system using the EKF.

Although the system uses the EKF or neural network to solve for controller gains at any linearized operating point, this is not the same as a full flight engine controller. At each operating point, the controller increments or decrements the control variables about their steady-state values, which must be solved using the Newton–Raphson method.[15]

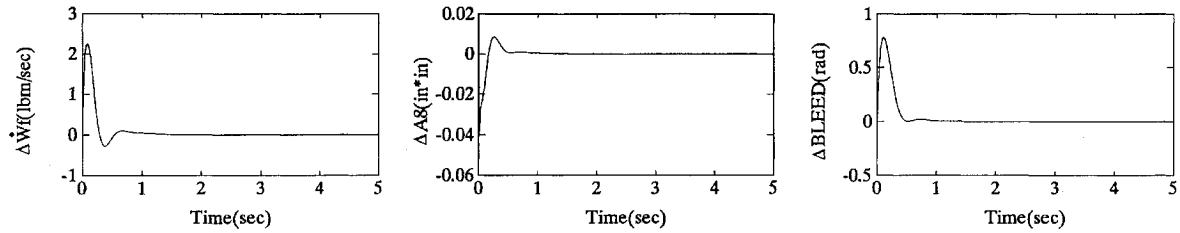

Main fuel flow Nozzel jet area Fan guide vane

Fig. 8 Controller outputs for test point 1 using EKF.

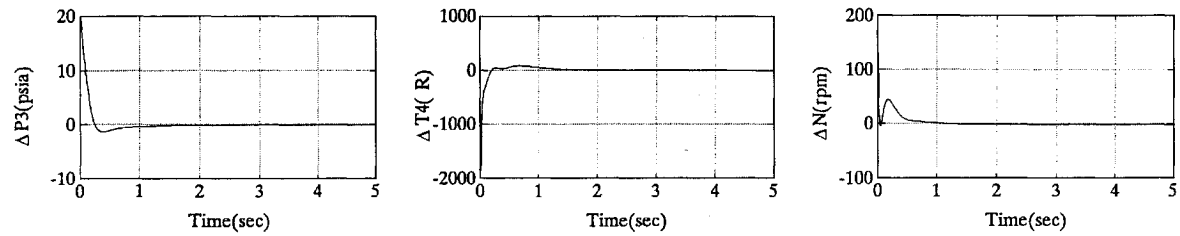

Pressure of compressor Fan turbine inlet temperature Shaft speed

Fig. 9 Closed-loop response of the outputs for test point 1 using neural network.

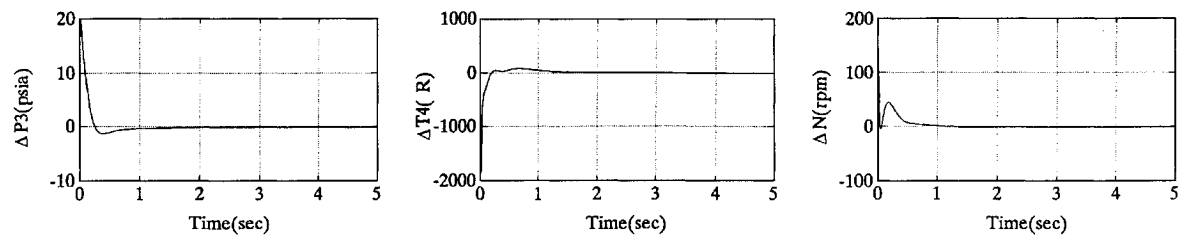

Pressure of compressor Fan turbine inlet temperature Shaft speed

Fig. 10 Closed-loop response of the outputs for test point 2 using neural network.

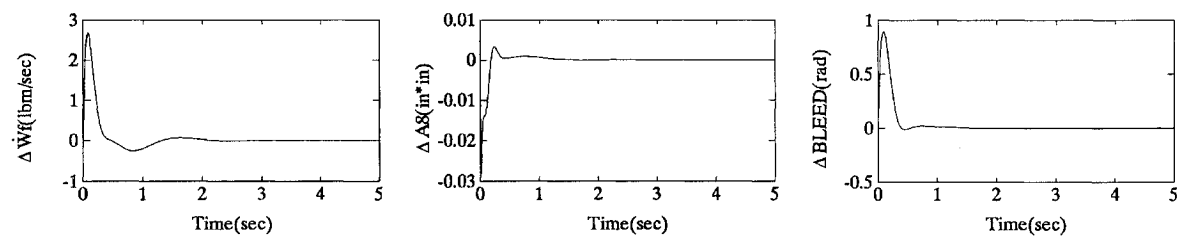

Main fuel flow Nozzel jet area Fan guide vane

Fig. 11 Controller outputs for test point 1 using neural network.

Conclusion

Edmunds' method is conceptually simple and easy to use. This method, however, does not guarantee that a satisfactory controller can be found. If the controller designed at the first trial does not meet the performance requirements, designers must modify a design step, such as the desired transfer function or the structure of the controller, until a satisfactory controller is found.

The performance of the system using a neural network scheduling method is better than that using an EKF scheduling method. The reason for this phenomenon is that we do not have to assume any particular function between the controller's gains and scheduled variables in neural networks as we do in the EKF.

Acknowledgment

This work was supported by the National Science Council, Taiwan, Republic of China, under Grant NSC 84-2212-E-005-001.

References

[1]Dehoff, R. L., Earl, H. W., Adams, R. J., and Gupta, N. K., "F-100 Multivariable Control Synthesis Program, Vol. 1, Development of F-100 Control System," NASA TP, AFAPL-TR-77-35, June 1977.

[2]Pfeil, W. H., Athans, M., and Spang, H. A., "Multivariable Control of the GE T700 Engine Using the LQG/LTR Design Methodology," American Control Conf., Seattle, WA, June 1986.

[3]Athans, M., Kapasouris, P., Kappos, E., and Spang, H. A., III, "Linear-Quadratic Gaussian with Loop-Transfer Recovery Methodology for the F-100 Engine," *Journal of Guidance, Control, and Dynamics*, Vol. 9, No. 1, 1986, pp. 45–52.

[4]Polley, J. A., Adibhatla, S., and Baheti, K. S., "Design of Jet Engine Control System by Multivariable Frequency-Domain Method," American Control Conf., Seattle, WA, June 1986.

[5]Edmunds, J. M., "Control System Design and Analysis Using Closed-Loop Nyquist and Bode Arrays," *International Journal of Control*, Vol. 30, No. 5, 1979, pp. 773–802.

[6]Moellenhoff, D. E., Vittal Rao, S., and Skarvan, C. A., "Design of Robust Controllers for Gas Turbine Engines," *Journal of Engineering for Gas Turbines and Power*, Vol. 113, April 1991, pp. 283–289.

[7]Kapasouris, P., "Gain-Scheduling Multivariable Control for the GE-21 Turbofan Engine Using the LQR and LQG/LTR Methodologies," S.M. Thesis, Dept. of Electrical Engineering and Computer Science, Massachusetts Inst. of Technology, Cambridge, MA, May 1984.

[8]Polley, J. A., Adibhatla, S., and Hoffman, P. J., "Multivariable Turbofan Engine Control for Full Flight Envelope Operation," *Journal of Engineering for Gas Turbines and Power*, Vol. 111, June 1989, pp. 130–137.

[9]Baker, W. L., and Farrell, J. A., "Learning Augmented Flight Control for

High Performance Aircraft," *Proceedings of the AIAA Guidance, Navigation, and Control Conference*, Vol. 1, AIAA, Washington, DC, 1991, pp. 653–663.

[10]Burgin, G. H., and Schnetzler, S. S., "Artificial Neural Networks in Flight Control and Flight Management System," *Proceedings of the IEEE National Aerospace and Electronics Conference* (Dayton, OH), Inst. of Electrical and Electronics Engineers, New York, 1990, pp. 567–573.

[11]Troudet, T., Garg, S., and Merrill, W. C., "Neural Network Approach to AIAA Aircraft Control Design Challenge," *Proceedings of the AIAA Guidance, Navigation, and Control Conference*, Vol. 3, AIAA, Washington, DC, 1991, pp. 993–1009.

[12]Narendra, K. S., and Parthasarathy, K., "Identification and Control of Dynamical Systems Using Neural Networks," *IEEE Transactions on Neural Networks*, Vol. 1, No. 1, 1990, pp. 4–27.

[13]Maciejowski, J. M., *Multivariable Feedback Design*, Addison–Wesley, Reading, MA, 1989.

[14]Doyle, J. C., and Stein, G., "Multivariable Feedback Design: Concepts for a Classical/Modern Synthesis," *IEEE Transactions on Automatic Control*, Vol. AC-26, No. 1, 1981, pp. 4–16.

[15]Hwang, C. H., "The Simulation of Performance for a Single Spool Turbojet Engine," M.S. Thesis, Dept. of Mechanical Engineering, National Chung-Hsing University, Taichung, Taiwan, ROC, 1994.

[16]Zurada, J. M., *Introduction to Artificial Neural Systems*, West Info Access, Singapore, 1992.